ELSEVIER

Physica B 308–310 (2001) 1137–1140

PHYSICA B

www.elsevier.com/locate/physb

Resonance ultrasonic diagnostics of defects in full-size silicon wafers

A. Belyaev, S. Ostapenko*

Center for Microelectronics Research, University of South Florida, 4202 E Fowler Avenue, Tampa, FL 33620, USA

Abstract

A resonance acoustic effect was observed recently in full-size 200 mm Cz-Si wafers and applied to characterize as-grown and process-induced defects. Ultrasonic vibrations can be excited into wafers using an external ultrasonic transducer and their amplitude is recorded using a scanning air-coupled acoustic probe operated in a non-contact mode. By sweeping driving frequency, f, of the transducer, we observed an amplification of a specific acoustic mode referred to as 'whistle'. In this paper, we performed theoretical modeling of the whistle which allowed in attributing this mode to resonant flexural vibrations in a thin circular plate. We calculated normal frequencies of the flexural vibrations of a circular plate of radius ρ in the case of the free edge. The model gives an excellent fit to experimental data with regard to whistle spatial distribution. The results of calculation allow the evaluation of resonance acoustic effect in wafers of different geometries employed in the industry. © 2001 Elsevier Science B.V. All rights reserved.

Keywords: Cz-Si; Ultrasonic; Vibrations

1. Introduction

The elastic stress in Cz-Si wafers and thin films can be caused by point defects and their complexes. For instance, thermal oxide on Cz-Si creates a residual stress of a few hundreds of MPa in the films due to a difference in thermal expansion of the substrate and oxide, which can be detrimental for gate-oxide integrity and reliability of CMOS devices. Residual elastic stress can also be harmful to silicon substrates, especially, with scaling of wafer diameter up to 300 mm. On the other hand, the stress can be a driving force to various types of defect reactions, such as precipitation of residual impurities deteriorating the electronic quality of material. Therefore, a problem of non-contact and non-destructive monitoring of residual stress/strain in as-grown, oxidized and epitaxial (Cz-Si) wafers is a current issue for microelectronics. Resonance acoustic diagnostics was developed and employed recently to characterize internal stress in full-size 200 mm Cz-Si wafers [1]. We report here the theoretical analysis of the resonance acoustic effect and compare calculation results with experimental data.

2. Experiment

Ultrasonic vibrations were generated into single-side polished Cz-Si wafers of 200 mm diameter using circular resonance piezoelectric transducer pressed by vacuum against the backside of the wafer [1]. These vibrations are propagated in the wafer beyond the transducer and form standing waves at specific frequencies. The amplitude of the standing wave is measured using an air-coupled acoustic probe. Fig. 1 demonstrates a frequency curve of the acoustic oscillations of Cz-Si wafer measured at probe location of 1 mm above the wafer front surface. By tuning driving frequency, f, of the transducer, we observed amplification of a specific acoustic mode referred to as 'whistle'. By changing the ac driving voltage we

*Corresponding author. Tel.: +1-813-974-2031; fax: +1-813-974-3610.

E-mail address: ostapenk@eng.usf.edu (S. Ostapenko).

0921-4526/01/$ - see front matter © 2001 Elsevier Science B.V. All rights reserved.
PII: S0921-4526(01)00914-0

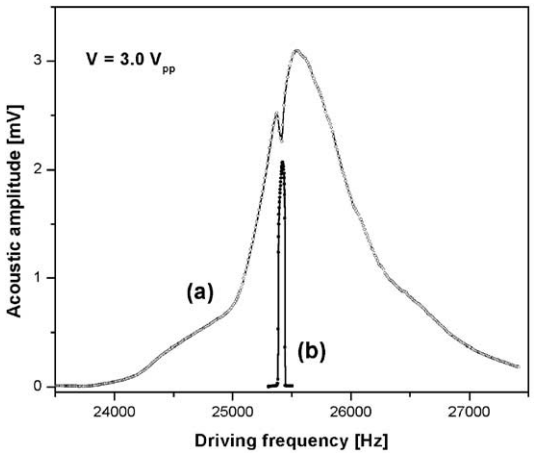

Fig. 1. Frequency scans of the transducer (a) and the whistle mode (b). The later is recorded with lock-in tuned to the half of driving frequency.

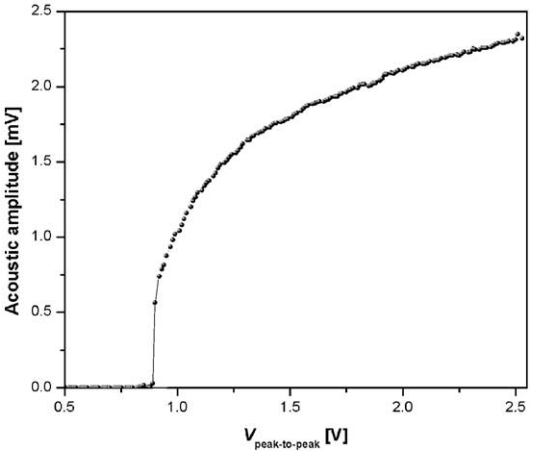

Fig. 2. Amplitude dependence of the whistle mode versus the voltage applied to transducer.

measured an amplitude scan of the acoustic signal. The amplitude scan shows a clear threshold as illustrated in Fig. 2, which is dependent on wafer history [2]. The characteristics of the whistle allow the attribution of this mode to resonance flexural vibrations in a thin circular plate.

3. Modeling

We consider flexural vibrations in a thin circular plate with thickness h and radius $\rho(h \ll \rho)$, which is a good model of a full-size 200 mm Cz-Si wafer. The equation for flexural vibrations can be represented as follows:

$$(\nabla^2\nabla^2 - \beta^4)u = 0, \tag{1}$$

where ∇^2 is the Laplace operator applied to u, and $\beta^4 = \omega^2\rho^4 h\xi/D$ is a dimensionless variable which depends on vibration frequency (ω), thickness and diameter of the wafer and flexural rigidity $D = Eh^2/12(1 - \nu^2)$, where E and ν, here, are Young's modulus and Poisson coefficient, respectively, and ξ is a density of material [3]. For flexural vibrations, we look for the solutions of the Eq. (1) in the form

$$U(\rho, \varphi) = u(\rho)e^{i\omega\varphi}, \tag{2}$$

where u is a normal displacement of a plate from equilibrium and ρ and φ are radial and polar coordinates with respect to the wafer center. Using the method of the separation of variables, one can obtain the general solution of Eq. (1) in the form

$$u(\rho, \varphi) = [aJ_n(\beta\rho) + bI_n(\beta\rho)]\begin{Bmatrix} \sin n\varphi \\ \cos n\varphi \end{Bmatrix}, \tag{3}$$

where J_n are Bessel functions and I_n are modified Bessel functions of the order n, respectively. Zero value of elastic stress components at the wafer edge ($\rho = 1$) leads to the free-edge boundary conditions

$$\left[\frac{2(\lambda+\mu)}{\lambda+2\mu}\frac{\partial}{\partial\rho}\nabla^2 u + \frac{\partial^3 u}{\partial\rho\,\partial\varphi^2} - \frac{\partial^2 u}{\partial\varphi^2}\right]\Bigg|_{\rho=1} = 0,$$
$$\left(\frac{\lambda}{\lambda+2\mu}\nabla^2 u + \frac{\partial^2 u}{\partial\rho^2}\right)\Bigg|_{\rho=1} = 0, \tag{4}$$

where λ and μ are Lame's constants. All the above, allow the calculation of the deformation pattern of thin silicon plate, which performs flexural vibrations. Figs. 3a and b show a correlation between experimental and calculated maps of the acoustic energy, which is proportional to the square of the acoustic displacement.

In the experiment with (1 0 0) oriented 200 mm Cz-Si wafers we observe high order flexural vibrations with $n = 20$ (Fig. 3a). This number is a consequence of four-fold symmetry of the (1 0 0) crystal plane, which permits $n = 4\,\mathrm{m}$ ($m = 1, 2, 3, \ldots$) values of the index n. Note that ρ is multiplied by a scale factor of 100, in order to raise it over to the experimental wafer's size. There is a clear similarity between the experimental and theoretical maps, especially at wafer periphery. One should mention that the additional maxima in the internal part of the experi-mental acoustic map are probably caused by a superposition of the major Bessel function of $n = 20$ with lower order solutions of Eq. (1), such as $n = 12$, 16, etc, satisfying $n = 4\,\mathrm{m}$ criterion. What is more important is that, according to our calculations, the lower order solutions shift the maximum of the radial distribution toward the wafer center, as illustrated by arrows in Fig. 4a.

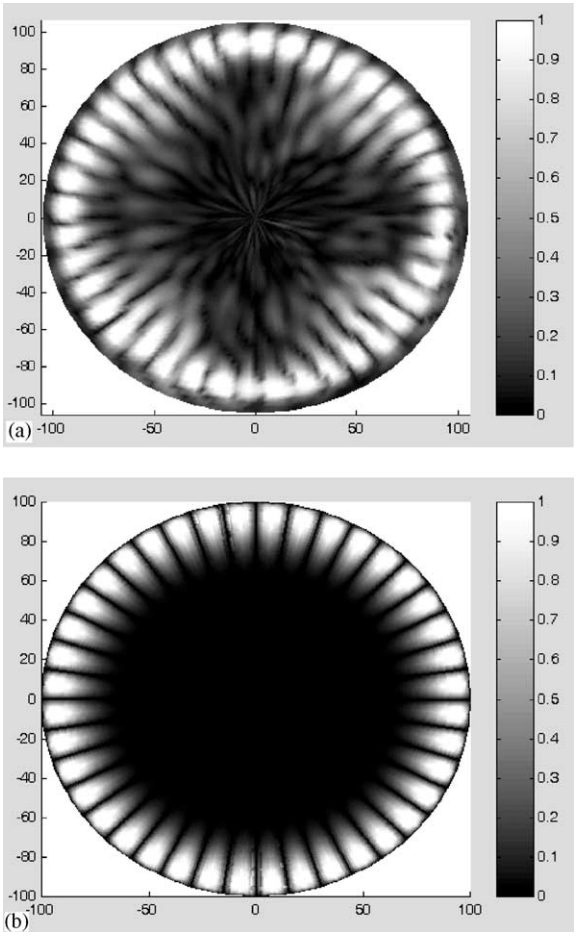

Fig. 3. (a)—acoustical map of the 'whistle' measured on 200 mm Cz-Si wafer at $\omega = 12.7$ kHz, $V = 2.8$Vpp. (b)—theoretical map of the high-order flexural vibrations of thin elastic plate with $n = 20$.

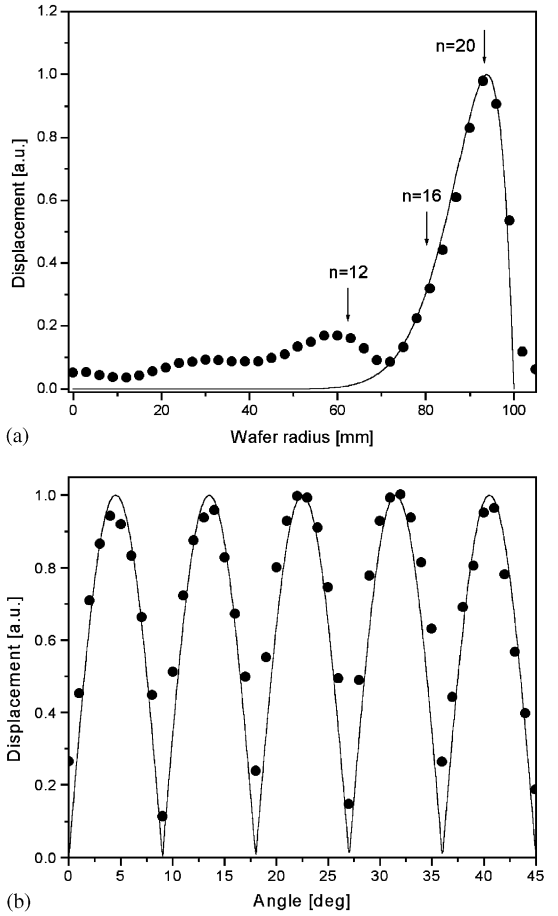

Fig. 4. Experimental distribution of the acoustic power (points) and theoretical fit (solid line) for (a) radial and (b) angular dependencies. Arrows on the radial scan indicate the positions of resonance flexural modes of different orders.

By separating variables in Eq. (1), we fit experimental data for radial and angular part individually. An illustrative example is presented in Figs. 4a and b. The angular curve fits the data with $\sin^2\varphi$ function. The radial curve shows a very good fit for the main maximum located at the wafer periphery. We notice that the experimental radial distribution of the flexural vibrations (Fig. 4a), shows additional lower index Bessel modes ($n = 12$) as we discussed earlier. Substituting (3) into (4) one can obtain the system of linear equations for coefficients a and b.

$$\begin{pmatrix} -\beta^3 J_n'(\beta) + (1-\nu)n^2[J_n(\beta) - \beta J_n'(\beta)] & \beta^3 I_n'(\beta) + (1-\nu)n^2[I_n(\beta) - \beta I_n'(\beta)] \\ -\beta^2 J_n(\beta) + (1-\nu)[n^2 J_n(\beta) - \beta J_n'(\beta)] & \beta^2 I_n'(\beta) + (1-\nu)[n^2 I_n(\beta) - \beta I_n'(\beta)] \end{pmatrix} \times \begin{pmatrix} a \\ b \end{pmatrix} = \begin{pmatrix} 0 \\ 0 \end{pmatrix}. \quad (5)$$

The frequency equation can be expressed by the condition that the determinant of the system vanishes. The normal (resonance) frequencies of flexural vibrations can be calculated using the equation [3]

$$\omega_{nm} = \frac{\beta_{nm}^2 h}{\rho^2}\sqrt{\frac{\mu}{6(1-\nu)\xi}}. \quad (6)$$

Fig. 5 illustrates the three sets of normal frequencies versus an order of Bessel's function for wafer diameters 150, 200, and 300 mm, which are mainly used in microelectronics. The dashed line indicates the resonant frequency observed in our experiment with 200 mm Cz-Si wafers. It shows that in the case of 200 mm diameter, one should expect flexural

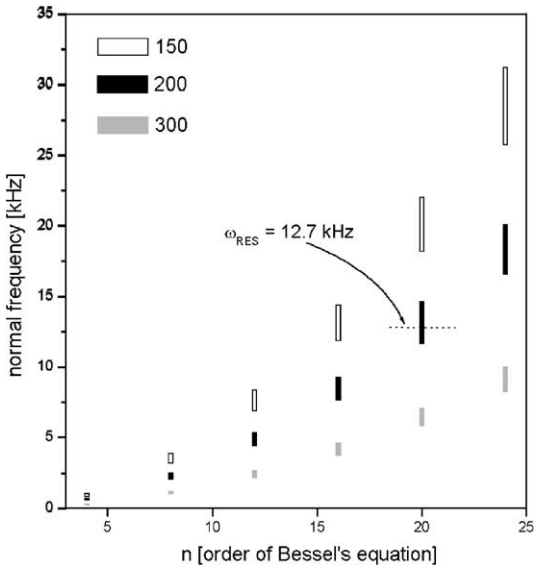

Fig. 5. Normal frequencies of the high-order flexural vibrations in silicon wafers of three diameters. The bars represent the effect on the frequencies the anisotropy of elastic modulus in silicon in $\langle 1\,0\,0 \rangle$, $\langle 1\,1\,1 \rangle$ and $\langle 1\,1\,0 \rangle$.

vibrations at the wafer periphery with $n = 20$. The bars at each Bessel mode n represent anisotropy of the elastic modulus in Si single crystals along $\langle 1\,0\,0 \rangle$, $\langle 1\,1\,0 \rangle$ and $\langle 1\,1\,1 \rangle$ crystallographic directions. The results of this modeling allow the prediction of a resonance acoustic effect in wafers of different geometry, crystallography, and other chemical origin employed by the electronic industry (GaAs, InP).

References

[1] S. Ostapenko, I. Tarasov, Appl. Phys. Lett. 76 (2000) 2217.
[2] A. Belyaev, V. Kochelap, I. Tarasov, S. Ostapenko, Characterization and Metrology for ULSI Technology, International Conference, 2000, pp. 207–211.
[3] K.C. Le, Vibrations of Shells and Rods, Springer, Berlin, 1999, pp. 89–95.